

# The Vitruvian Baby: Interactive Reformation of Fetal Ultrasound Data to a T-Position

Eric Mörth<sup>1,2,3</sup> , Renata G. Raidou<sup>2</sup> , Ivan Viola<sup>2,4</sup>  and Noeska N. Smit<sup>1,3</sup> 

<sup>1</sup>Department of Informatics, University of Bergen, Norway

<sup>2</sup>Institute of Visual Computing & Human-Centered Technology, Vienna University of Technology, Austria

<sup>3</sup>Mohn Medical Imaging and Visualization Centre, Haukeland University Hospital, Norway

<sup>4</sup>Computer, Electrical and Mathematical Science and Engineering Division, King Abdullah University of Science and Technology, Saudi Arabia

---

## Abstract

Three-dimensional (3D) ultrasound imaging and visualization is often used in medical diagnostics, especially in prenatal screening. Screening the development of the fetus is important to assess possible complications early on. State of the art approaches involve taking standardized measurements to compare them with standardized tables. The measurements are taken in a 2D slice view, where precise measurements can be difficult to acquire due to the fetal pose. Performing the analysis in a 3D view would enable the viewer to better discriminate between artefacts and representative information. Additionally making data comparable between different investigations and patients is a goal in medical imaging techniques and is often achieved by standardization. With this paper, we introduce a novel approach to provide a standardization method for 3D ultrasound fetus screenings. Our approach is called “The Vitruvian Baby” and incorporates a complete pipeline for standardized measuring in fetal 3D ultrasound. The input of the method is a 3D ultrasound screening of a fetus and the output is the fetus in a standardized T-pose. In this pose, taking measurements is easier and comparison of different fetuses is possible. In addition to the transformation of the 3D ultrasound data, we create an abstract representation of the fetus based on accurate measurements. We demonstrate the accuracy of our approach on simulated data where the ground truth is known.

## CCS Concepts

• **Applied computing** → **Health informatics**; • **Human-centered computing** → **Visualization design and evaluation methods**;

---

## 1. Introduction

Ultrasound imaging and visualization are commonly used in medical fetus diagnostics [HZ17, VBS\*13]. Analysis based on two dimensional (2D) images is common in clinical environments and especially in ultrasound screening [LCEC09]. Loughna et al. [LCEC09] describe fetal size measurement and dating techniques and introduce recommended charts. In order to date the pregnancy and to assess the development of the fetus, the overall growth is an important measurement. The crown rump length (CRL) and the head circumference (HC) are shown to be of great interest in this regard [LCEC09]. Loughna et al. [LCEC09] state that the circumferences are not measured directly, but they are calculated, using the length and the width measured in a 2D slice view. A big challenge in medicine is to achieve comparability between patients and between investigations. Standardization and normalization is one solution that addresses this problem and has been applied to different kinds of diagnostic applications [NUX02]. Gynecologists have to face the challenge of aligning the measurement plane perfectly with the object of interest e.g. the femur of the fetus while coping with the large variety of fetal poses [FH89]. Using 3D ultrasound instead of 2D would enable taking measurements after

the screening without having to perform the alignment [VBS\*13]. The images and also the volumetric data cannot be compared directly between screenings of different timepoints or different fetuses without standardization.

With this work, we propose standardization in terms of prenatal 3D ultrasound investigations. Our main contribution is a novel, comprehensive pipeline to transform 3D ultrasound data of a fetus to a standardized T-pose in a semi-automatic way, to automatically take accurate measurements and visually compare growth patterns with average growth values. Our workflow is called “Vitruvian Baby” and provides an interface not only for the standardization of the fetal position, but also for the exploration of the measurements taken from the standardized result. Furthermore, we introduce an abstract representation of the fetus which enables fast and accurate comparison between the automatically taken measurements and standardized growth information.

## 2. Related Work

Ultrasound is an acoustical investigation that is susceptible to various noise-induced artifacts. Therefore, Solteszova et al. [SBS\*17] introduced a filtering to regions of the volume which have a poten-

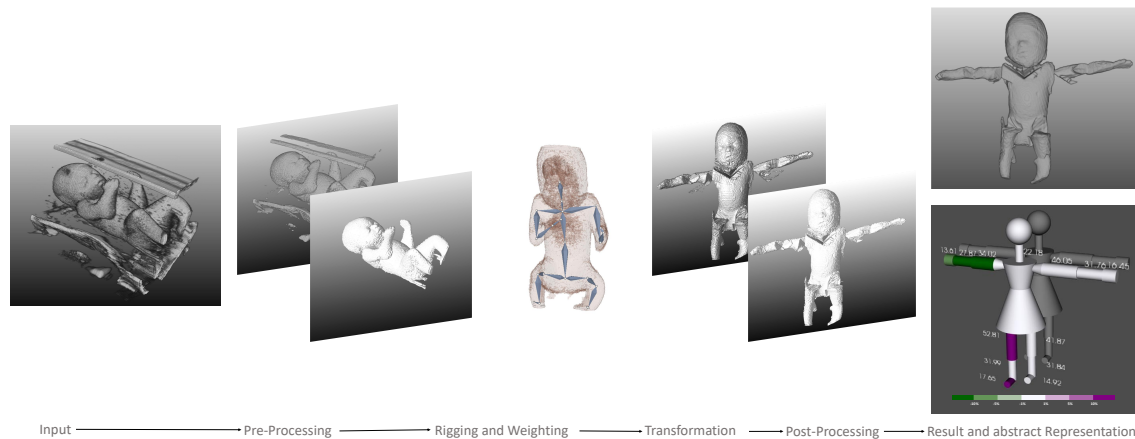


**Figure 1:** The Vitruvian Baby workflow from left to right: The input of the workflow consists of 3D ultrasound screening data of a fetus, which is afterwards pre-processed to segment the fetus. Then the rigging and weighting is performed before transforming the fetus to a T-pose. Post-processing is applied to reduce artifacts and to obtain a clean result. In addition, the result is presented in an abstract way including automatically created measurements, to support comparability

tial effect on the image. The volumetric area which is perceivable during an ultrasound investigation is limited, therefore, techniques to generate compound volumes on the fly are important [VBS\*13]. Bagci et al. [BUB10] stated that standardization describes techniques that can be used in order to cope with inter- and intra-subject variations. Miao et al. [MMNG15] proposed that the usage of an abstract version of the data provides more insight and comparability, and introduced a standardized representation of the Circle of Willis, a circulatory anastomosis that supplies blood to the brain. Miao et al. [MMK\*17] also presented a technique to visualize the MRI imaging data of the in utero placenta in a standardized way.

**Rigging and reformations** Shapiro et al. [SFW\*14] introduced an automatic rigging method using voxels. Bharaj et al. [BTST12] presented a procedure to automatically rig a character by using a joint mapping technique based on point clouds and clustering. These approaches assume a standardized pose as an input and are therefore not applicable in our context. Manual rigging is the process of defining the position of a predefined skeleton or armature in a mesh or volume. Finet et al. [FOA\*14] introduced Bender, an open source 3D Slicer [PHK04] extension that provides tools for efficient rigging, weighting, model posing and morphing. Magnenat-Thalmann et al. [MTLT88] proposed a linear blend skinning technique, where a heat distribution plot is created between the segments of the armature, which is used to define which voxels are affected by a movement of the given segment. This type of weighting is also implemented in Bender [FOA\*14] and used in our workflow. Kreiser et al. [KMM\*18] discussed different approaches for bone based reformations in their survey. Raidou et al. [RCMA\*18] presented Blade Runner, a flattening and unfolding approach to visually analyze correlation. Raidou et al. [GKGR18] also introduced a technique to analyze distortions of volumes. Providing an abstract representation of complex spatial data is a way to reduce information overload and potentially reduce analysis time.

In general, related work provides different approaches that could be adapted for our purposes, but does not provide an integrated solution which can address the entire workflow from the pre-processing to the identification of unnatural growth patterns

through measurements. The presented rigging and weighting approaches are only sparsely applicable for the voxel data provided by ultrasound screening. Standardized views on the 3D ultrasound data of the fetus can provide comparability between screenings on different timepoints or between different fetuses, which is the main purpose of introducing “The Vitruvian Baby“. As an additional form of standardization, we introduce an abstract representation of the fetus aimed at making the measurement data comparable and easily understandable at a glance.

### 3. The Vitruvian Baby

The Vitruvian Baby is a workflow that enables the transformation of the data of a 3D ultrasound screening of a fetus to a standardized T-pose. Furthermore, it provides an abstract representation of the fetus, including the measurements and the deviation from standard growth. Figure 1 visualizes the complete workflow. The workflow takes the result of a 3D ultrasound screening of a fetus as input data. First, the data is pre-processed to segment the fetus in the data, then the fetus is rigged and weighted. The next step is to transform the data to a T-pose. Due to the fact that artifacts may occur during the transformation, the post-processing pipeline aims to clean the result. In addition to the transformed fetal ultrasound data, an abstract representation of the fetus, including measurements, is created. The abstract representation provides another form of standardization and enables a neutral communication with the parents.

The first step is to *load the data*. Our workflow expects the voxel data of the 3D ultrasound screening as the input source data, including the whole fetus in a single acquisition. The *pre-processing pipeline* used in this application includes thresholding to distinguish between background data and the data belonging to the fetus. A largest connected component analysis using a 3D 18-neighborhood is performed to extract the fetus. *Rigging* is performed using Bender, as presented by Finet et al. [FOA\*14]. The “armature” module of the software can be used to create and place an armature in a model. After considering different approaches, we chose to perform this step in a manual way involving user interaction, in order to incorporate domain knowledge into the rig-

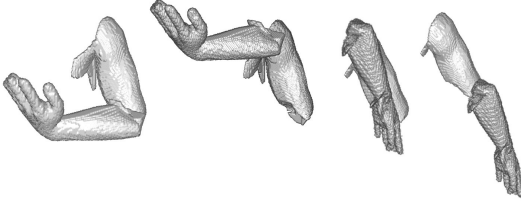


**Figure 2:** From left to right: the initial arm pose, the forearm with the same origin of the coordinate system as the upper arm, the result after the rotation of the forearm in the same direction as the upper arm, and the result after performing the transformation around the connection point between the upper arm and the forearm.

ging process. The *weighting* of the data is performed using Bender [FOA\*14]. The output of this step is a volume which includes the mapping for each voxel to one of the armature segments. We used a linear blend skinning approach for the weighting of the voxels. The weighting may be adjusted manually, e.g., in case of extremities touching the body of the fetus, where voxels belonging to the torso are linked to armature parts of the extremities and would be difficult to separate.

**Transformation** The transformation is performed automatically based on armature and volume input. First the volume is split into the parts that will be transformed by using the weighting information. The basic idea of the approach is to transform each segment of the armature with respect to the segment it is attached to. In some special cases, such as the leg transformation, a rotation is performed in the direction of the spine instead of the attached segment, which would be the hips. In order to visualize this transformation process, the left arm of a model is shown in the example visible in Figure 2. The visualization of the initial pose is the first picture in Figure 2. First the forearm is shifted to the head of the left upper arm. This amounts to positioning the coordinate system to the head of the left upper arm. The shift is visible in the second image of Figure 2. The result of the transformation in this example should be that the forearm faces directly in the same direction as the upper arm. First, we need to obtain the axis of rotation, and secondly, we need to calculate the angle between the two vectors, representing the forearm and the upper arm. The angle of rotation is calculated by  $a = u \times v / \|u \times v\|$ , where  $u$  and  $v$  are the two vectors and  $a$  is the axis of rotation. The angle between the vectors is then calculated by  $\alpha = \arccos(u \cdot v)$ . Based on this information, one can calculate the rotation matrix about this arbitrary axis using the information provided by McDonald [McD06]. Before representing the rotation matrix, two further calculations have to be made, namely  $c = \cos(\alpha)$  and  $s = \sin(\alpha)$ . The rotation matrix is presented in Equation 1:

$$M_r = \begin{bmatrix} a_x^2(1-c) + c & a_x a_y(1-c) - a_z s & a_x a_z(1-c) + a_y s \\ a_x a_y(1-c) + a_z s & a_y^2(1-c) + c & a_y a_z(1-c) - a_x s \\ a_x a_z(1-c) - a_y s & a_y a_z(1-c) + a_x s & a_z^2(1-c) + c \end{bmatrix} \quad (1)$$

McDonald states that  $a$  should be a unit vector, because the matrix would not represent a rotation if this is not the case [McD06]. The equation  $v_r = M_r u$  calculates the rotation of a vector to point in the same direction as a given goal vector. Applying the rotation matrix to the given example, we obtain the third image in Figure 2. In this image, also the hand has been rotated in direction of the

forearm in the same way as described. The fourth image of Figure 2 shows the result after shifting the forearm and the hand back to the connection point between the upper arm and the forearm. The artefacts visible in this example originate from the weighting of the voxels.

The next step consists of the *post-processing* of the results. We apply a largest connected component analysis. This step aims to remove artifacts that do not belong to the fetus. Another step applied in the post-processing is a filtering step to make the result look smoother. We chose a Gaussian smoothing with a  $\sigma$  value of 1.0. Other possible values may range from 0.5 to 2.5, depending on how much detail should be preserved.

The last step of the pipeline is the *analysis*, which has the aim to obtain insight from the transformed data. In addition, The Vitruvian Baby workflow includes the creation of an abstract representation of the fetus. The representation includes the measurements of the extremities as well as the neck, as shown in Figure 3. It also displays comparison to standard growth patterns of the fetus. To this end, we use a puppet representation consisting of cylinders, cones and spheres. The measurements are presented as numbers in millimeters beside the corresponding elements. Due to the fact that the transformed fetus data in a T-pose includes artifacts and does not reflect a natural depiction of a fetus the puppet also enables an neutral communication with the parents and an additional standardization of the fetus.

In order to provide meaningful arrangements of the puppets presenting the actual and a standard growth of the fetus, we used the techniques described by Gleicher et al. [GAW\*11]. We decided to encode the measurements of the fetus explicitly in the abstract representation, i.e., the length of the different geometric objects is proportional to the measured length of the representing parts of the fetus. To enable the comparison between the actual measurements of the fetus and the average growth we used two different comparison techniques, namely juxtaposition and superposition. We provide two possibilities for the juxtaposition technique. One presents the average growth as a gray puppet posterior or behind the puppet representing the fetus as shown in the first image of Figure 3. The other option is to place the average growth puppet lateral from the fetus puppet, as presented in the middle image of Figure 3. We also support comparison via superposition, which we achieve by showing a silhouette of the average growth superimposed on the fetal puppet representation, visualized in the right image of Figure 3.

In addition to the spatial comparison techniques, we use color as an additional channel to encode deviation from standard growth. We use a diverging and discrete colormap from dark green to white to dark purple with seven categories, as is shown in Figure 3. Standard growth is encoded as white, larger growth is represented by purple, while smaller growth is visible as green. The deviation from the standard growth is categorized into three categories per deviation type. We chose the category borders to represent the usual confidence intervals of 99%, 95% and 90% in one-sided confidence intervals. These are then mapped to one color each. We chose a deviation of 1% larger or smaller to be in the normal range. Between 1% and 5% is the first level of deviation, between 5% and 10% the second, and larger or smaller than 10% constitutes the most extreme variation from the average.

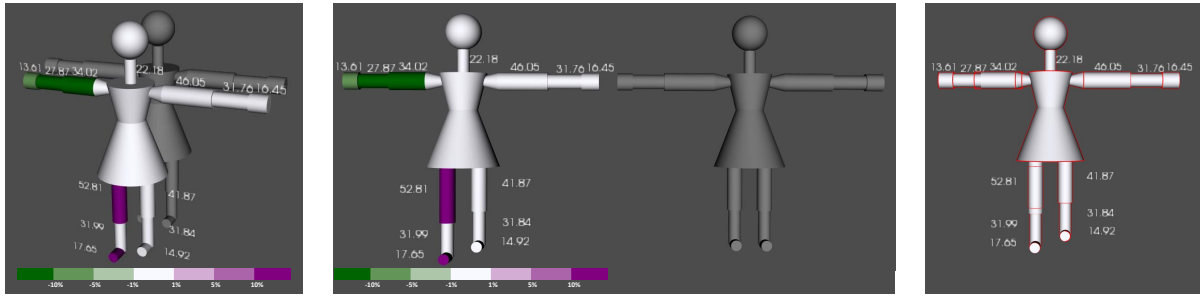


**Figure 3:** From left to right: the representation of the fetal measurements with color encoding the deviation from the average in front and standard growth in gray, the measurements and the standard growth side by side, and the abstract presentation with the standard growth as a silhouette outline.

**4. Results**

We use a model of a human given in a T-pose to validate our method quantitatively and qualitatively, and in addition also apply our approach to a phantom 3D ultrasound screening of a fetus. The model of the human can be transformed into different fetus-like poses using Blender [Fou19] and is available online, licensed by the Royalty Free License [Squ10]. Blender works with a surface representation of the 3D models, therefore a voxelized model has to be created, e.g., by using the *stl-to-voxel* Python script introduced by Pederkoff [Ped15]. The head is affected by some artifacts which occurred during the mesh to voxel transformation. As the measurements taken from the fetus have to be precise and correct, we measure the performance of the approach by calculating the similarity of the head to toe measurement, and the span measurement from finger to finger between the resulting T-pose and the original T-pose. In order to determine the average result accuracy, we tested our workflow on seven different poses to resemble positions in the womb [FH89]. The results are shown as a bar chart diagram in Figure 4 for comparison. Figure 4 also shows all the poses that have been used for testing as well as the resulting T-pose. The average finger to finger span measurement similarity is 91,08% and the similarity of the head to toe measurement is even higher at 94,05%.

**Fetus phantom** In addition to validating our approach on model data, we also applied our approach on a phantom 3D ultrasound screening of a fetus, which is displayed in Figure 1. The dataset provided by Cortes et al. [CKM\*16] unfortunately does not include the feet in the ultrasound acquisition. First, we applied a filtering with a threshold function where all values greater than 60 are used. The next step is a largest connected component filtering where we removed detached particles from the dataset. The result after this step is shown in the third image of Figure 1. After the rigging, weighting, and transformation, we apply a post-processing procedure. The result after the first and the second step of the post-processing is presented in the fifth and sixth image of Figure 1. The Gaussian smoothing with a  $\sigma$  of 1 creates the result shown on the top right in Figure 1. The abstract representation of the fetus is shown in Figure 3. In order to show the functionality of the representation, we prepared a sample dataset representing an irregular growth of the right side of the fetus. As shown in Figure 3, the right upper arm, forearm, and hand of the fetus are too short. In addition, the right femur and the right foot are too long. All the other segments of the fetus are within a normal range of growth. The results show that

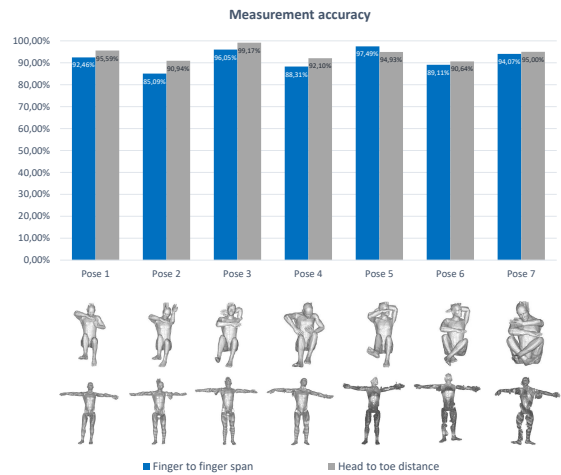


**Figure 4:** Chart representing the finger to finger measurement similarity in blue and the head to toe measurement similarity in gray, between the result of the method and the ground truth. The legend shows the input pose and the results of our method.

the accuracy of the unfolding in terms of measurement precision is quite high but there are artifacts included in the data after the unfolding. Therefore the standardized puppet representation may be more suitable for a parent doctor communication.

**5. Conclusion and Future Work**

We presented an approach for the transformation of fetal ultrasound investigation data to a standardized pose and the generation of an abstract representation of fetal measurements. Standardization was already introduced in several areas of medical imaging [MMNG15, OGH\*06, NUX02], and in case of fetal screening, it would enable longitudinal and latitudinal comparison of fetal development. The measurements of the fetus are taken automatically after the transformation. The transformation of the surface of the fetus, gathered by mesh generating algorithms would possible lead to more visual appealing results, but would also result in losing details of the data. We assessed the performance of our solution by using model data where the ground truth is known [Squ10], as well as a phantom ultrasound acquisition [CKM\*16]. The process of rigging can be very tedious, therefore a semi-automatic approach might be an improvement. A domain expert should get the opportunity to

have a look at the rigging result, and if needed, he or she should be able to adapt the positioning of the segments and joints in the data. In the future, we would also like to conduct an extensive evaluation with clinical users. The domain knowledge of gynecologists, radiologists, and also radiographers would be beneficial to further refine our approach and adapt the tool adequately. As it stands, The Vitruvian Baby workflow allows standardized measurements in 3D fetal ultrasound with the goal of improving growth analysis and comparison between multiple acquisitions and standard growth.

## Acknowledgments

This research was partially supported by the Trond Mohn Foundation (grant number '811255').

## References

- [BTST12] BHARAJ G., THORMÄHLEN T., SEIDEL H. P., THEOBALT C.: Automatically rigging multi-component characters. *Computer Graphics Forum* 31, 2 (2012), 755–764. doi:10.1111/j.1467-8659.2012.03034.x. 2
- [BUB10] BAĞCI U., UDUPA J. K., BAI L.: The role of intensity standardization in medical image registration. *Pattern Recognition Letters* 31, 4 (2010), 315–323. doi:10.1016/j.patrec.2009.09.010. 2
- [CKM\*16] CORTES C., KABONGO L., MACIA I., RUIZ O. E., FLOREZ J.: Ultrasound image dataset for image analysis algorithms evaluation. In *Innovation in Medicine and Healthcare*. Springer, 2016, pp. 447–457. URL: [http://link.springer.com/10.1007/978-3-319-23024-5\\_41](http://link.springer.com/10.1007/978-3-319-23024-5_41), doi:10.1007/978-3-319-23024-5(\\_}41. 4
- [FH89] FERGUSON J. H., HAULTAIN F. W. N.: Handbook of obstetric nursing. In *Handbook of Obstetric Nursing*. Young J. Pentland in Edinburgh, 1889, pp. 150–153. URL: [https://openlibrary.org/books/OL26302696M/Handbook\\_of\\_obstetric\\_nursing.1,4](https://openlibrary.org/books/OL26302696M/Handbook_of_obstetric_nursing.1,4)
- [FOA\*14] FINET J., ORTIZ R., ANDRUEJOL J., ENQUOBAHRIE A., JOMIER J., PAYNE J., AYLWARD S.: Bender: An Open Source Software for Efficient Model Posing and Morphing. In *Biomedical Simulation*. Springer, 2014, pp. 203–210. URL: [http://link.springer.com/10.1007/978-3-319-12057-7\\_23](http://link.springer.com/10.1007/978-3-319-12057-7_23), doi:10.1007/978-3-319-12057-7(\\_}23. 2, 3
- [Fou19] FOUNDATION S. B.: Blender, 2019. URL: <https://www.blender.org/>. 4
- [GAW\*11] GLEICHER M., ALBERS D., WALKER R., JUSUFI I., HANSEN C. D., ROBERTS J. C.: Visual comparison for information visualization. *Information Visualization* 10, 4 (Oct. 2011), 289–309. URL: <http://dx.doi.org/10.1177/1473871611416549>, doi:10.1177/1473871611416549. 3
- [GKGR18] GROSSMANN N., KÖPPEL T., GRÖLLER M. E., RAIDOU R.: Visualflatter - visual analysis of distortions in the projection of biomedical structures. *Eurographics Proceedings* (Sept. 2018). URL: <https://www.cg.tuwien.ac.at/research/publications/2018/raidou2018visualflatter/>. 2
- [HZ17] HUANG Q., ZENG Z.: A review on real-time 3d ultrasound imaging technology. *BioMed Research International* 2017 (03 2017), 1–20. doi:10.1155/2017/6027029. 1
- [KMM\*18] KREISER J., MEUSCHKE M., MISTELBAUER G., PREIM B., ROPINSKI T.: A Survey of Flattening-Based Medical Visualization Techniques. *Computer Graphics Forum* 37, 3 (2018), 597–624. doi:10.1111/cgfm.13445. 2
- [LCEC09] LOUGHNA P., CHITTY L., EVANS T., CHUDLEIGH T.: Fetal size and dating: Charts recommended for clinical obstetric practice. *Ultrasound* 17, 3 (2009), 160–166. URL: <http://journals.sagepub.com/doi/10.1179/174313409X448543>, doi:10.1179/174313409X448543. 1
- [McD06] McDONALD J.: Rotation About an Arbitrary Axis. In *CGEMS - Computer Graphics Educational Materials* (18-7-2006), (Ed.), The Eurographics Association. doi:10.2312/cgems04-11-1367. 3
- [MMK\*17] MIAO H., MISTELBAUER G., KARIMOV A., ALANSARY A., DAVIDSON A., LLOYD D. F. A., DAMODARAM M., STORY L., HUTTER J., HAJNAL J. V., RUTHERFORD M., PREIM B., KAINZ B., GRÖLLER M. E.: Placenta maps: In utero placental health assessment of the human fetus. *IEEE Transactions on Visualization and Computer Graphics* 23, 6 (June 2017), 1612–1623. doi:10.1109/TVCG.2017.2674938. 2
- [MMNG15] MIAO H., MISTELBAUER G., NASEL C., GRÖLLER M. E.: Cowradar: Visual quantification of the circle of willis in stroke patients. In *EG Workshop on Visual Computing for Biology and Medicine* (Sept. 2015), Bühler K., Linsen L., John N. W., (Eds.), EG Digital Library, The Eurographics Association, pp. 1–10. URL: [https://www.cg.tuwien.ac.at/research/publications/2015/Miao\\_2015\\_VCBM/](https://www.cg.tuwien.ac.at/research/publications/2015/Miao_2015_VCBM/). 2, 4
- [MTLT88] MAGNENAT-THALMANN N., LAPERRIÈRE R., THALMANN D.: Joint-Dependent Local Deformations for Hand Animation and Object Grasping. *Proceedings on Graphics Interface '88* (1988), 26–33. 2
- [NUX02] NYUL L., UDUPA J., XUAN ZHANG: New variants of a method of MRI scale standardization. *IEEE Transactions on Medical Imaging* 19, 2 (2002), 143–150. URL: <http://ieeexplore.ieee.org/document/836373/>, doi:10.1109/42.836373. 1, 4
- [OGH\*06] OELTZE S., GROTHUES F., HENNEMUTH A., KUSS A., PREIM B.: Integrated visualization of morphologic and perfusion data for the analysis of coronary artery disease. *Eurographics/IEEE VGTC Symposium on Visualization*, June 2014 (2006), 131–138. URL: [papers2://publication/uuid/C574B865-6478-4351-B3C6-B9851F649529](https://papers2://publication/uuid/C574B865-6478-4351-B3C6-B9851F649529), doi:10.2312/VisSym/EuroVis06/131-138. 4
- [Ped15] PEDERKOFF C.: stl-to-voxel, 2015. URL: <https://github.com/cpederkoff/stl-to-voxel.4>
- [PHK04] PIEPER S., HALLE M., KIKINIS R.: 3D Slicer. In *2004 2nd IEEE International Symposium on Biomedical Imaging: Nano to Macro (IEEE Cat No. 04EX821)* (April 2004), vol. 1, pp. 632–635. doi:10.1109/ISBI.2004.1398617. 2
- [RCMA\*18] RAIDOU R., CASARES-MAGAZ O., AMIRKHANOV A., MOISEENKO V., MUREN L. P., EINCK J. P., VILANOVA A., GRÖLLER M. E.: Bladder runner: Visual analytics for the exploration of rt-induced bladder toxicity in a cohort study. *Computer Graphics Forum* 37, 3 (2018), 205–216. URL: [https://www.cg.tuwien.ac.at/research/publications/2018/raidou2018\\_bladderrunner/](https://www.cg.tuwien.ac.at/research/publications/2018/raidou2018_bladderrunner/), doi:10.1111/cgfm.13413. 2
- [SBS\*17] SOLTESZOVA V., BIRKELAND Å., STOPPEL S., VIOLA I., BRUCKNER S.: Output-Sensitive Filtering of Streaming Volume Data. *Computer Graphics Forum* 36, 1 (2017), 249–262. doi:10.1111/cgfm.12799. 1
- [SFW\*14] SHAPIRO A., FENG A., WANG R., LI H., BOLAS M., MEDIONI G., SUMA E.: Rapid avatar capture and simulation using commodity depth sensors. *Computer Animation and Virtual Worlds* 25, 3-4 (2014), 201–211. doi:10.1002/cav.1579. 2
- [Squ10] SQUIDIFIER T.: Detailed Man. <https://www.turbosquid.com/3d-models/free-obj-mode-human/544305>, 2010. The Squidifier. Accessed: 2019-04-12. 4
- [VBS\*13] VIOLA I., BIRKELAND Å., SOLTESZOVA V., HELLJESEN L., HAUSER H., KOTOPOULIS S., NYLUND K.: High-quality 3D visualization of in-situ ultrasonography. In *EuroGraphics —Dirk Bartz Prize* (2013), pp. 1–4. doi:10.2312/conf/EG2013/med/001-004. 1, 2